AD NUMBER

AD486847

NEW LIMITATION CHANGE

TO

Approved for public release, distribution unlimited

FROM

Distribution authorized to U.S. Gov't. agencies and their contractors; Administrative/Operational Use; 01 FEB 1966. Other requests shall be referred to Air Force Weapons Lab., Kirtland AFB, NM.

AUTHORITY

AFWL ltr, 30 Nov 1971

AD 486847

GENERAL DYNAMICS
General Atomic Division

SPECIAL NUCLEAR EFFECTS LABORATORY

P.O. BOX 608, SAN DIEGO, CALIFORNIA 92112

GAMD-7098
Category A

Copy No.

SHOCK TRANSMISSION THROUGH A SOLID-SOLID INTERFACE

Work done by:

J. K. Dienes
R. H. Fisher

Report written by:

J. K. Dienes
R. H. Fisher

This document, which was prepared primarily for internal use at General Atomic, may contain preliminary or incomplete data. It is informal and is subject to revision or correction; it does not, therefore, represent a final report.

Sponsored by
Advanced Research Projects Agency
ARPA Order No. 251
Monitored by
Air Force Special Weapons Center
Contract AF29(601)4759

Project 249
February 1, 1966

INTRODUCTION

When a plane shock wave moving through one material meets an interface with a new material, the shock is transmitted at a different strength into the "target" material and a new wave is reflected back into the "parent" material. The strength of the transmitted wave is determined in this report for the case when both materials are solid and can be described by a Mie-Gruneisen equation of state.

The reflected wave may be either a shock or a rarefaction. In the first case, the transmitted shock pressure exceeds that in the incident shock. This occurs generally, but not necessarily, when the target material is denser than the parent material. In the second case, the reflected rarefaction, there is a reduction in shock pressure. This situation arises typically, but not necessarily, when the target material is of lower density than the parent material. One result of this report is to exhibit the boundary between these two cases. This boundary can also be interpreted as the relation between bulk modulus and density in the target material such that there is no reflected wave and consequently all of the energy in the incident wave is transmitted.

This analysis was made to facilitate estimates of the damage incurred in structures which are strongly shocked, as from hypervelocity projectile impact, intensive x-ray exposure, or underground nuclear explosions. Actual failure of structural materials is incurred as a result of shock-wave reflection at either a free surface or at a contact surface. The resulting negative pressure could lead to tensile fracture and possibly spallation fragments. However, failure criteria will not be considered in this report.

REFLECTION OF ACOUSTIC WAVES

When a wave is sufficiently weak, whether tensile or compressive, it is referred to as an acoustic wave and its analysis can be carried out in considerable detail since the governing equations are linear. The general solution to the acoustic reflection problem is discussed separately in this section since an elementary analytical solution is available. The solution to the nonlinear shock reflection problem discussed in the body of this report has the acoustic solution of Eq.(1) as a limit when the shock pressures are well below the bulk modulus of the material. For the geometry outlined in Fig. 1, the ratio of the pressure after reflection, p_3, to the pressure before reflection, p_1, is

$$\frac{p_3}{p_1} = \frac{2}{1 + \rho_0\, c_0/\rho_2\, c_2} = \frac{2}{1 + (K_0\, \rho_0/K_2\, \rho_2)^{\frac{1}{2}}} , \tag{1}$$

where ρ is the density, c is the sound speed based on the bulk modulus, $c = \sqrt{K/\rho}$, K is the bulk modulus, and $\rho c = \sqrt{K\rho}$ is the acoustic impedance. The result given in Eq. (1) shows that the pressure ratio never exceeds 2 in the acoustic case.

The above result can be used to determine the pressure ratio for a wave transmitted through a slab of material embedded in a different material. If the subscripts 1 and 2 are used to denote the outside and inside materials, respectively, then the ratio of transmitted pressure, P_T, to incident pressure, P_I, is

$$\frac{P_T}{P_I} = \frac{4\, \rho_1\, c_1\, \rho_2\, c_2}{(\rho_1\, c_1 + \rho_2\, c_2)^2} . \tag{2}$$

$\rightarrow u_4$

Region 1	Region 3	Region 4	Region 2
Once-shocked Parent Material	Twice-shocked Parent Material	Once-shocked Target Material	Unshocked Target Material
p_1, u_1	$p_3 = p_4$, $u_3 = u_4$	p_4, u_4	$p_2 = u_2 = 0$
K_0, $\rho_1 = 1/V_1$	K_0, $\rho_3 = 1/V_3$	K_2, $\rho_4 = 1/V_4$	K_2, $\rho_2 = 1/V_2$

Reflected shock — Contact surface — Transmitted shock

Parent Material — Target Material

NOTE: A zero subscript, $(\ )_0$, denotes the state of unshocked parent material; although no such material appears in the figure, it will have bulk modulus K_0 and density ρ_0.

Fig. 1--Geometry for the shock reflection problem.

If the acoustic impedance ratio is as large as 10, or as small as 1/10, the pressure transmitted through the sandwich is 64% of the original. This is about the greatest reduction that might be expected with common materials. The effect of subsequent reflections within the sandwich may complicate the result for some applications.

REFLECTION OF SHOCKS IN IDEAL GASES

For ideal gases, the pressure ratio behind the reflected shock for the geometry of Fig. 1 is given by Courant and Friedrichs[1] where the target material is treated as a rigid wall:

$$\frac{p_3 - p_0}{p_1 - p_0} = 1 + \frac{\mu^2 + 1}{\mu^2 + p_0/p_1} , \tag{3}$$

where p_0 is the initial static pressure and $\mu^2 = (\gamma - 1)/(\gamma + 1)$ depends on γ, the ratio of specific heats. For strong shocks, this simplifies to

$$\frac{p_3 - p_0}{p_1 - p_0} = \frac{3\gamma - 1}{\gamma - 1} , \tag{4}$$

which is 8 for $\gamma = 7/5$ and 6 for $\gamma = 5/3$. For weak shocks, p_0/p_1 is near unity and the pressure ratio is near 2, as in the acoustic case when the target material has infinite acoustic impedance. Thus, the shock-reflection pressure ratios are larger in the ideal gas--strong shock case than in the acoustic case. It is this fact that motivated the work described here, since for strong shocks in solids it was not clear whether the large pressure ratios found in the perfect gas case or the small pressure ratios found in the acoustic approximation would be more nearly correct.

EQUATIONS FOR THE REFLECTED SHOCK CASE

The geometry for the general shock reflection problem is outlined in Fig. 1, which defines the four regions that appear in the shock-reflection problem. (Material in the initial state, denoted by a zero subscript, is not shown in Fig. 1.) The usual shock relations as given in Ref. 1, page 129, are:

$$\rho_1 v_1 = \rho_2 v_2 , \tag{5}$$

$$p_1 + \rho_1 v_1^2 = p_2 + \rho_2 v_2^2 , \tag{6}$$

$$p_1/\rho_1 + E_1 + \tfrac{1}{2} v_1^2 = p_2/\rho_2 + E_2 + \tfrac{1}{2} v_2^2 \tag{7}$$

where v_1 denotes the relative velocity of the material and the shock. In addition to these conservation equations, an equation of state of the Mie-Gruneisen form,

$$p = G(V)\, E/V + F(V) , \tag{8}$$

is assumed in order to complete the physical description of the problem. A review of the experimental data in Ref. 2 suggests that if the Gruneisen ratio G(V) has the form

$$G(V) = G_0\, V/V_0 , \tag{9}$$

then the data are in many instances fitted better than if G(V) is taken to be a constant. This assumption also leads to convenient analytical expressions in the calculation of isentropes. In the present analysis, G_0 is taken to be 2, which is typical, but not necessarily accurate, for most materials. The best choice of G_0 for various materials generally lies in the range from 1.5 to 3.0, but the final results appear insensitive to the value of G_0, as indicated in Fig. 2.

The determination of F(V) follows from the empirical observation[2] that the shock velocity, u_s, and the material velocity, u_p, behind a shock into a material at rest are related through the equation

$$u_s = c + S\, u_p . \tag{10}$$

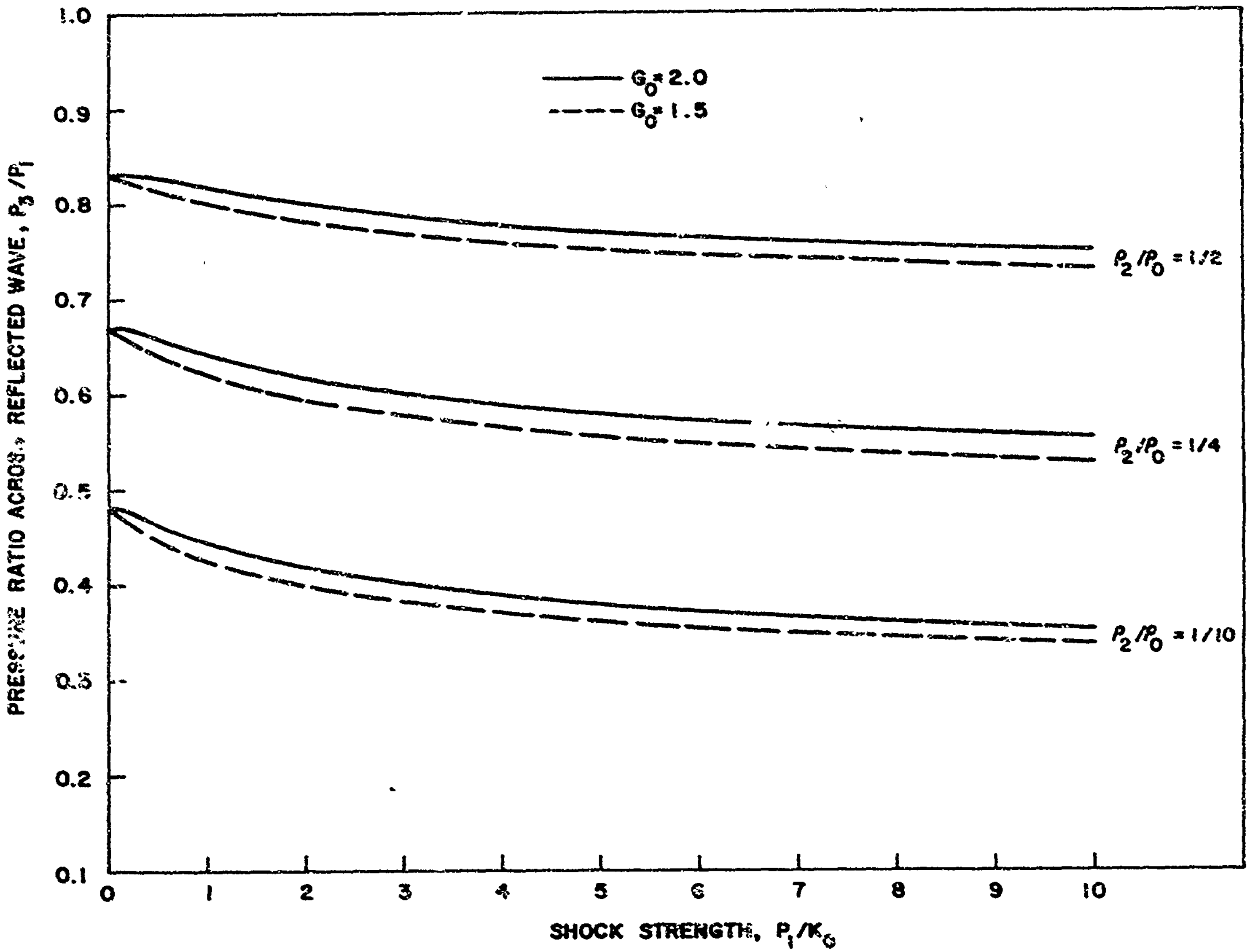

Fig. 2--The effect of variation in the constant G_0 on shock reflection pressures for equal bulk modulus, $K_2 = K_0$, and three values of density ratio.

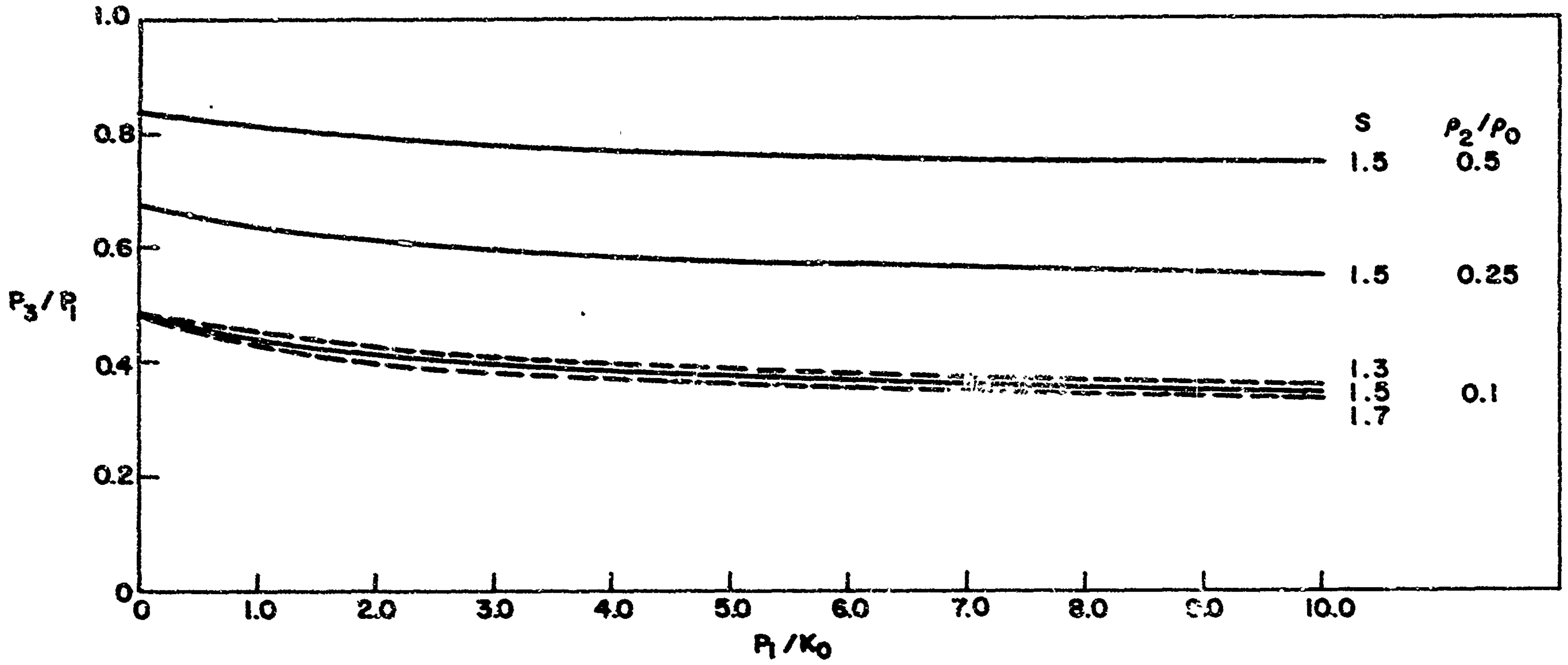

Fig. 3--The effect of variation in the parameter, S, appearing in $U_S = C_0 + SU_0$, the linear shock velocity-particle velocity relation of Ref. 2.

The empirical parameter, S, usually has values in the range from 1.2 to 2.0 and was taken to be 1.5 in the calculations. As with G_0, subsequent results appear insensitive to the value of S, as illustrated in Fig. 3. Combining this equation with the shock relations of Eqs. (5), (6), and (7) leads to

$$F(V) = K\theta(1 - G_0\,\theta/2)/(1 - S\theta)^2 = K\,f(\theta)\ ,\quad \theta = 1 - V/\overline{V} \tag{11}$$

where K is the bulk modulus of the material and $\overline{V}$ is the initial specific volume. Equations for the pressure and velocity in Region 4 behind the transmitted shock can be obtained from the first two shock equations, (5) and (6), in terms of the compression θ_4, where

$$\theta_4 = 1 - V_4/V_2\ . \tag{12}$$

(The initial specific volume, $\overline{V}$, is V_2 in this instance.) These relations are:

$$p_4 = K_2\,\frac{f(\theta_4)}{1 - G_0\,\theta_4/2} \tag{13}$$

and

$$u_4 = \sqrt{\theta_4\,p_4\,V_2}\ . \tag{14}$$

(It will be assumed that the Gruneisen ratio is the same in both materials.) A comparison of the shock pressure from Eq. (13) with the more detailed treatment by Tillotson in Ref. 3 is given in Fig. 4, which shows the Hugoniot for pressures up to 100 Mbar in copper. (Copper is a convenient example, since it has the selected values of $G_0 = 2$ and $S = 1.5$.)

Equations for the compression θ_3 and the pressure p_3 in Region 3 are obtained by considering the conservation equations across the reflected shock. The appropriate equations relating these conditions in Regions 3 and 1 are, after appropriate manipulations of Eqs. (5) through (9),

$$\theta_3 = \theta_1 + \frac{(u_3 - u_1)^2}{(p_3 - p_1)\,V_0}\ , \tag{15}$$

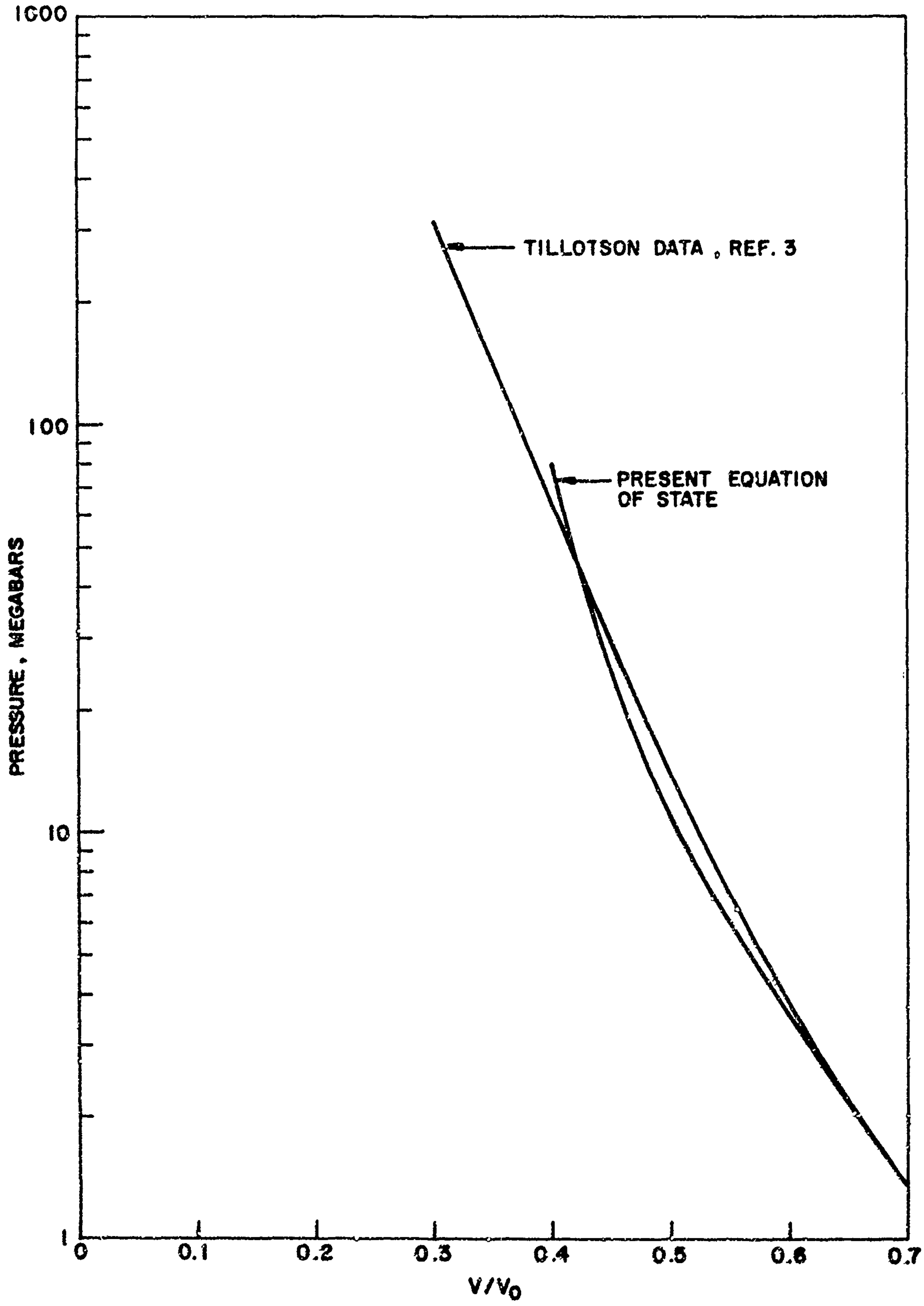

Fig. 4--Comparison of shock pressure in the low pressure approximation of Eqs. 11 and 12 with the more general Hugoniot of Ref. 3.

$$p_3 = \frac{p_1 \left[1 + G_0(\theta_3 - \theta_1)/2\right] + K_0\left[f(\theta_3) - f(\theta_1)\right]}{1 - G_0(\theta_3 - \theta_1)/2}\ , \tag{16}$$

where

$$\theta_3 = 1 - V_3/V_0\ , \qquad \theta_1 = 1 - V_1/V_0 \tag{17}$$

The additional requirement that the pressure and velocity be continuous between Regions 3 and 4 completes the formulation of the problem.

EQUATIONS FOR THE REFLECTED RAREFACTION CASE

Region 3 of Fig. 1 may contain a rarefaction wave under some conditions. If this is the case, the pressure will vary isentropically in that region, and it is necessary to have an equation relating pressure and specific volume on the isentrope. This is obtained by considering the equation of state

$$p = G_0 E/V_0 + F(V) . \tag{18}$$

In order that $dS = (dE + pdV)/T$ be a perfect differential, it is necessary that

$$\frac{\partial}{\partial V} \left(\frac{1}{T} \frac{\partial E}{\partial T}\right) = \frac{\partial}{\partial T} \left[\frac{1}{T} \left(p + \frac{\partial E}{\partial V}\right)\right]$$

or, substituting from the equation of state,

$$- E_V + T G_0 E_T / V_0 = G E/V_0 + F(V) ,$$

where the subscripts denote differentiation with respect to that variable. The characteristic equations[4] are

$$\frac{dV}{-1} = V_0 \frac{dT}{TG_0} = \frac{dE}{F(V) + G_0 E/V_0} .$$

Two independent solutions containing arbitrary constants c_1 and c_2 are obtained by combining the first equation with the second and then that equation with the third:

$$c_1 = H(V) + E e^{G_0 V/V_0} , \qquad \text{where } H(V) = \int_{V_0}^{V} e^{G_0 V/V_0} F(V) \, dV ,$$

$$c_2 = G_0 V/V_0 + \ln T ,$$

leading to the general solution

$$E = e^{- G_0 V/V_0} \left[- H(V) + J \left(T e^{G_0 V/V_0}\right)\right] \tag{19}$$

where J denotes an arbitrary function. H(V) is plotted in nondimensional form in Fig. 5 for the function given by Eq. (11). If the specific heat is assumed constant and equal to C_V, then

$$\frac{\partial E}{\partial T} = C_V = J'(T\, e^{G_0 V/V_0})$$

and therefore the function J must be linear in its argument. It follows that the equation of state is

$$E = C_V\, T - e^{-G_0 V/V_0} \int e^{G_0 V/V_0}\, F(V)\, dV \tag{20}$$

and the entropy is given by

$$S - S_0 = C_v \ln \left\{ \frac{E\, e^{G_0 V/V_0} + H(V)}{C_V\, T_0} \right\}, \tag{21}$$

where S_0 is an arbitrary constant. Combining this expression with the equation of state, the isentrope connecting the pressures in Regions 1 and 4 is given by

$$[p_1 - F(V_1)]e^{G_0 V_1/V_0} + G_0\, H(V_1)/V_0 = [p_3 - F(V_3)]e^{G_0 V_3/V_0} + G_0\, H(V_3)/V_0\,. \tag{22}$$

The Riemann integral[1] is used to find the relation between u and V along the particle paths. The appropriate solution for the current problem is

$$u_1 - u_3 = \int_{V_3}^{V_1} \frac{c\, dV}{V} = W(V_1) - W(V_3)\,. \tag{23}$$

The sound speed, c, appearing in the above integrand can be obtained from the equation

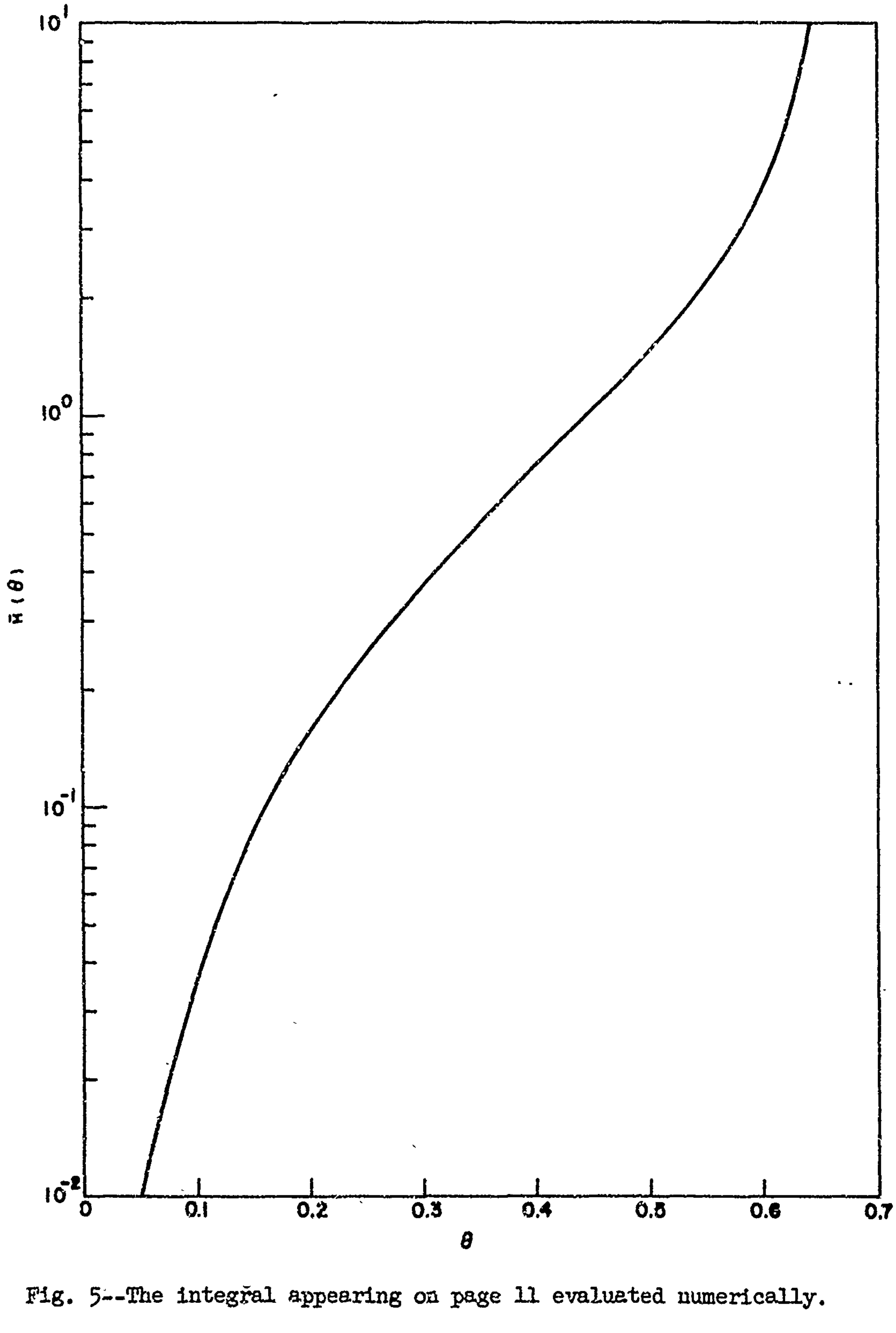

Fig. 5--The integral appearing on page 11 evaluated numerically.

$$\frac{c}{V} = \sqrt{-\left(\frac{\partial p}{\partial V}\right)_S} = \sqrt{-F_V + G_0\, p/V_0} \tag{24}$$

and the expression below for the pressure on an isentrope from the point (V_3, p_3) in the p-V plane:

$$p = F(V) + e^{-G_0 V/V_0} \left\{ G_0\,[H(V) - H(V_3)]/V_0 + [p_3 - F(V_3)]\, e^{G_0 V_3/V_0} \right\} . \tag{25}$$

CALCULATIONS

The equations for shock transmission were solved by an iteration technique using the IBM-7040. A general outline of the solution procedure is given in the flow diagrams on the two following pages. The calculations were done using nondimensional pressures and velocities, which are denoted by bars. The following list relates the quantities in the flow diagram to those used in the theoretical discussions above.

$$\bar{p}_1 = p_1/K_0 \qquad \bar{p}_2 = p_2/K_2 \qquad \bar{p}_3 = p_3/K_0 , \qquad \bar{p}_4 = p_4/K_2$$

$$\bar{u}_1 = u_1/c_0 \qquad \bar{u}_2 = u_2/c_2 \qquad \bar{u}_3 = u_3/c_0 , \qquad \bar{u}_4 = u_4/c_2$$

$$c_0^{\,2} = K_0/\rho_0 \qquad\qquad c_2^{\,2} = K_2/\rho_2$$

$$\bar{H}(\theta) = H(V)/K_0 , \qquad \theta = 1 - V/V_0 .$$

$$\bar{W}(\theta) = \frac{1}{c_0} W(V)$$

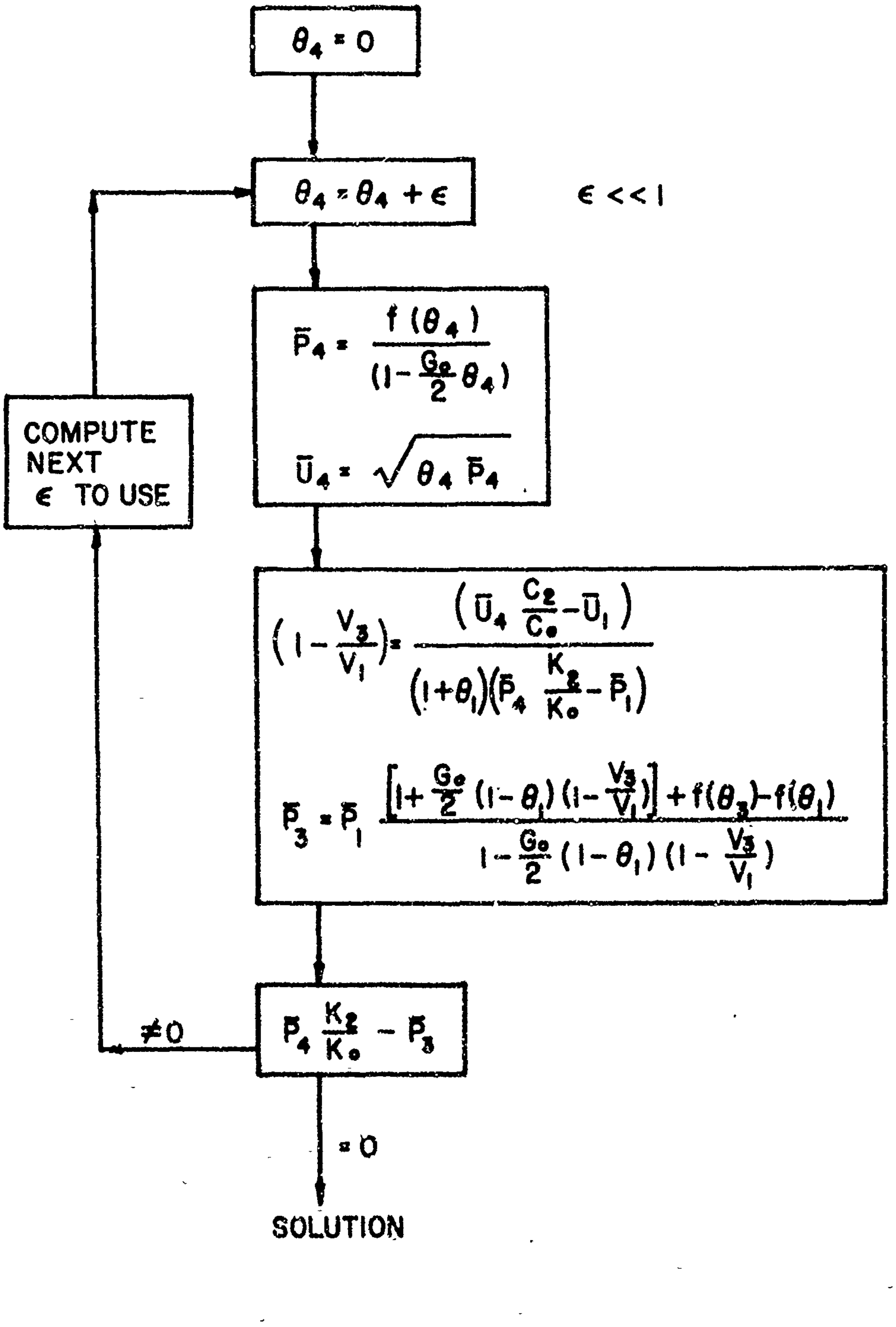

Chart 1. Solution procedure for the reflected shock.

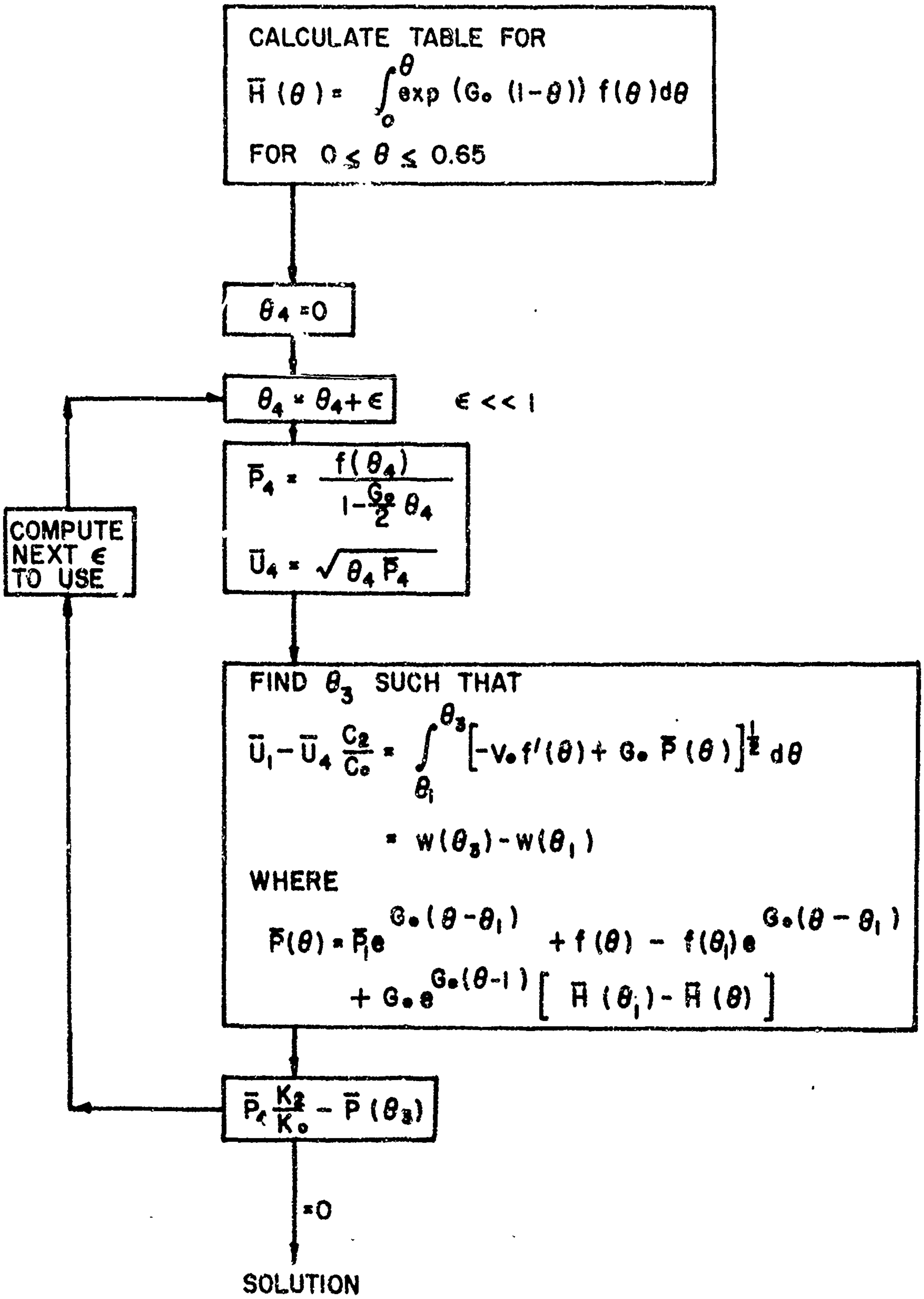

Chart 2. Solution procedure for the reflected rarefaction.

SUMMARY AND CONCLUSIONS

The purpose of this report is to provide a survey of the pressure ratios, p_3/p_1, encountered in the shock reflection process. In Figs. 6-12 the results of the calculations are given for initial shock pressures in the range from zero to ten times the bulk modulus, with both the density and bulk modulus ratios being varied in the two materials. When the transmitted pressure is less than that in the incident wave, the reflected wave is a rarefaction, and when it exceeds that in the incident wave, the reflected wave is a shock. The curves for the two cases fit smoothly together, as might be expected on theoretical grounds, by noting that when the pressure ratio is near unity the reflected wave is weak, and thus the Hugoniot and isentropes for the reflected wave have a third-order contact.[(1)] The pressure ratios lie between 1/3 and 3 in the region of the parameters investigated, which includes bulk modulus and density ratios from 1/10 to 10. The velocity ratios, u_3/u_1, are plotted in Figs. 13 through 19.

The "complete transmission" curves separating the reflected shock case from the reflected rarefaction case are shown in Fig. 20 as a relation between bulk modulus ratio, K_2/K_0, and density ratio, ρ_2/ρ_0. This relation depends on shock strength. When the shock is weak, the complete transmission curve is given by acoustic theory and is $K_2\rho_2 = K_0\rho_0$. As the incident shock strength is increased, the curve separating the two cases approach the line $\rho_2/\rho_0 = 1$. Thus for strong shocks complete transmission requires only that the density ratio be near unity. The density ratio is therefore more important than the bulk modulus in determining the transmitted shock pressures for strong shocks. This is to be expected on physical grounds, since at higher pressures materials begin to behave as a gas and the bulk-modulus terms in the Mie-Gruneisen equation become relatively small.

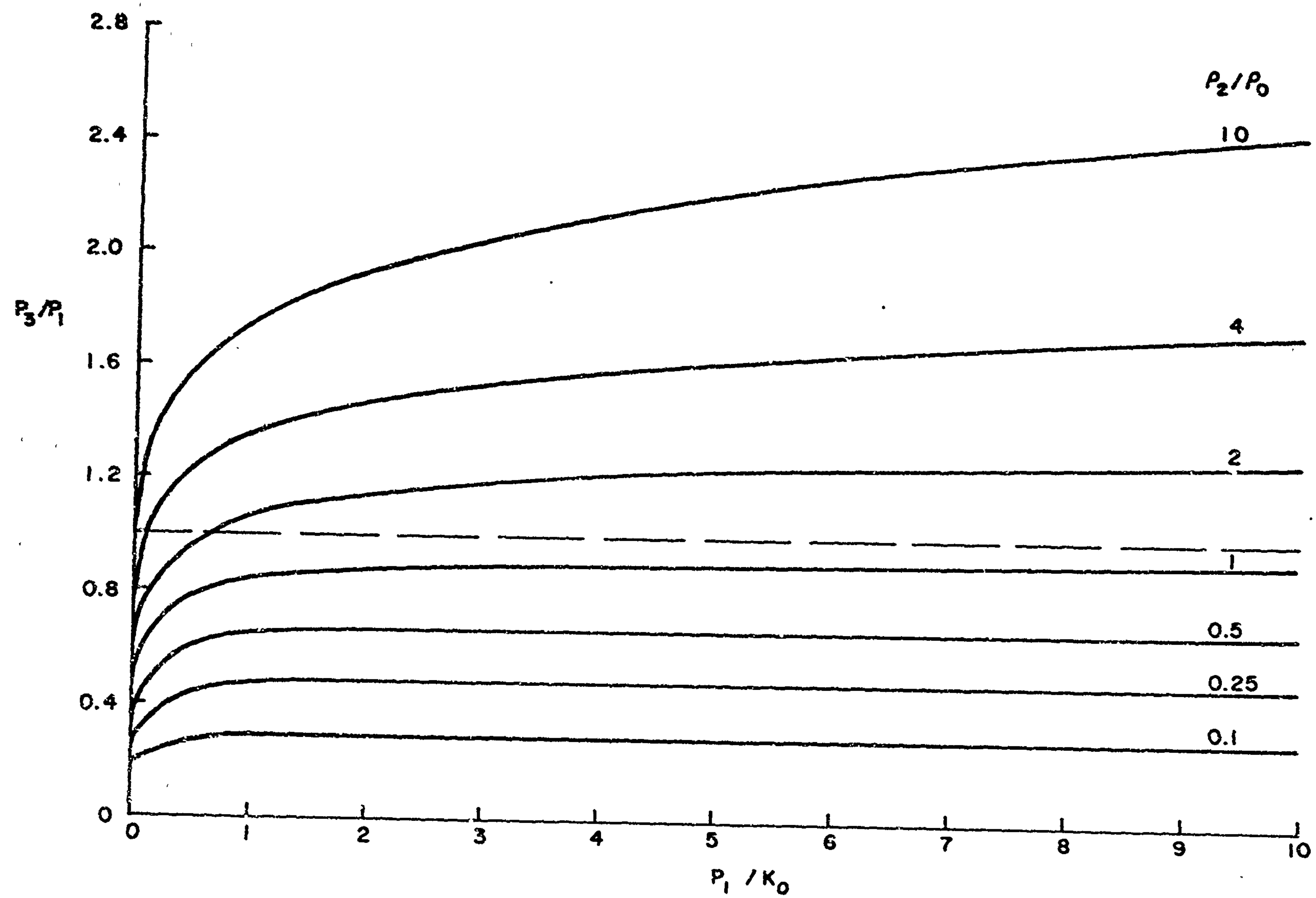

Fig. 6--The ratio of transmitted pressure, p_3, to incident pressure, p_1, in the case where the bulk modulus ratio, K_2/K_0 equals 1/10.

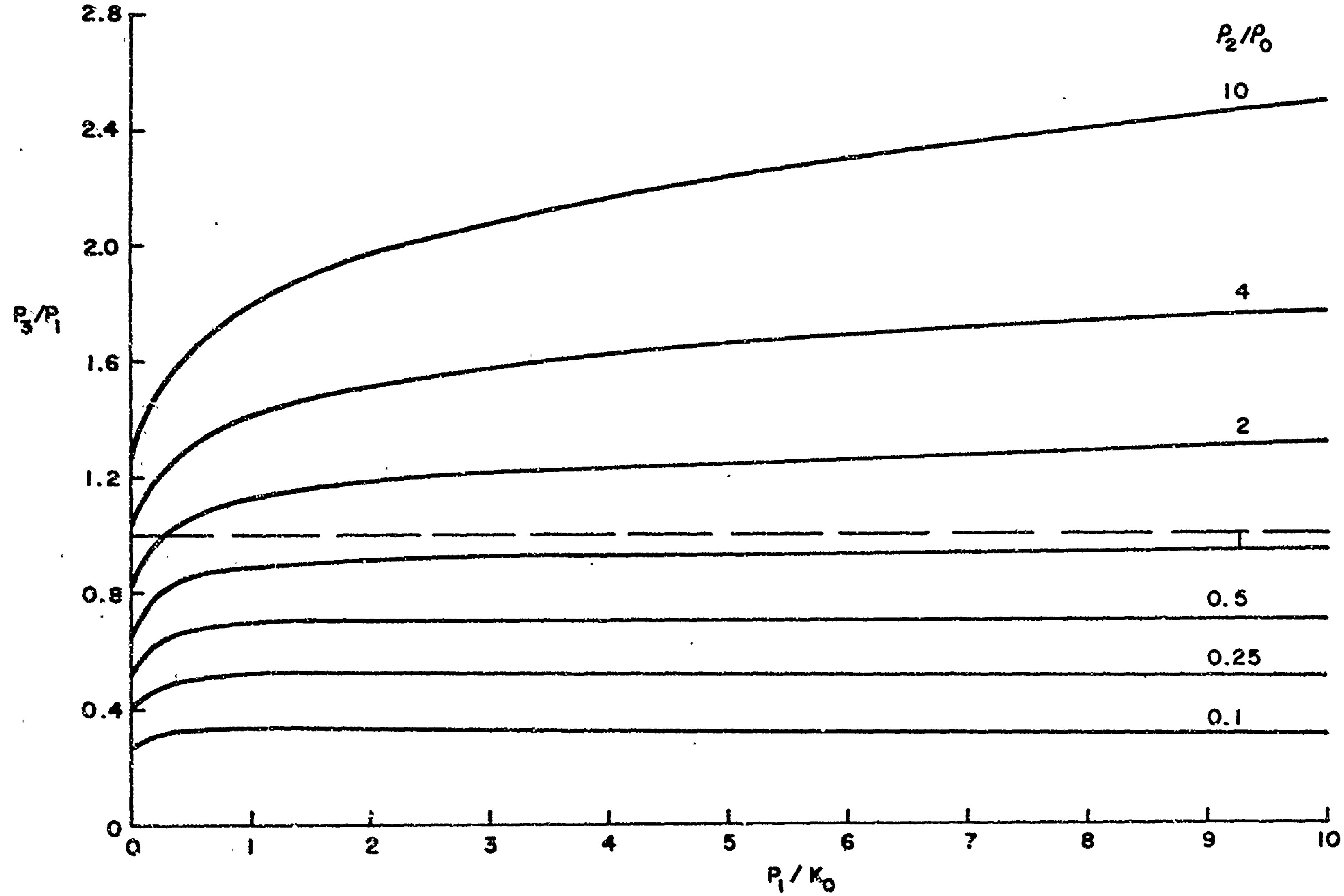

Fig. 7--The ratio of transmitted pressure, p_3, to incident pressure, p_1, in the case where the bulk modulus ratio, K_2/K_0 equals 1/4.

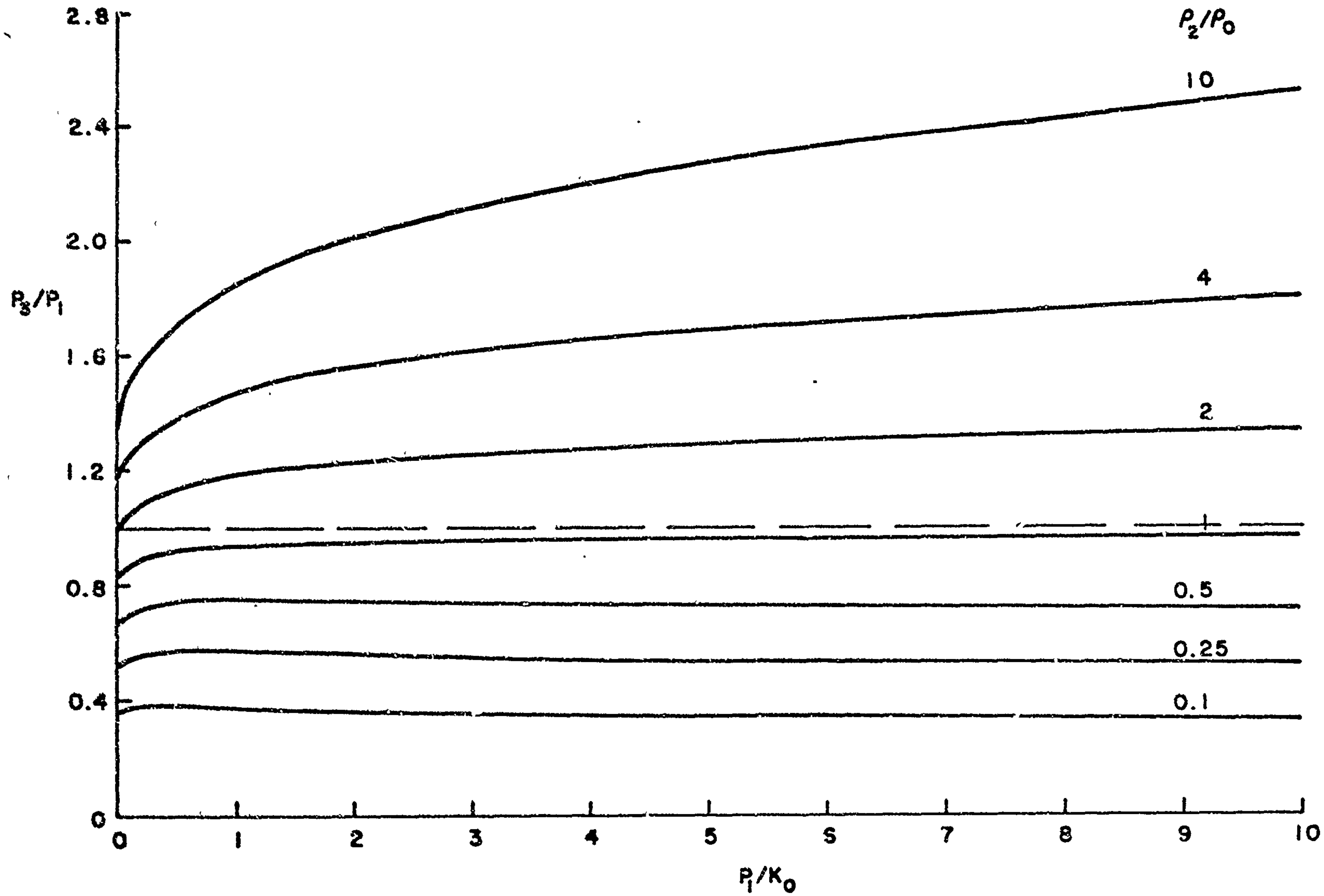

Fig. 8--The ratio of transmitted pressure, p_3, to incident pressure, p_1, in the case where the bulk modulus ratio, K_2/K_0 equals 1/2.

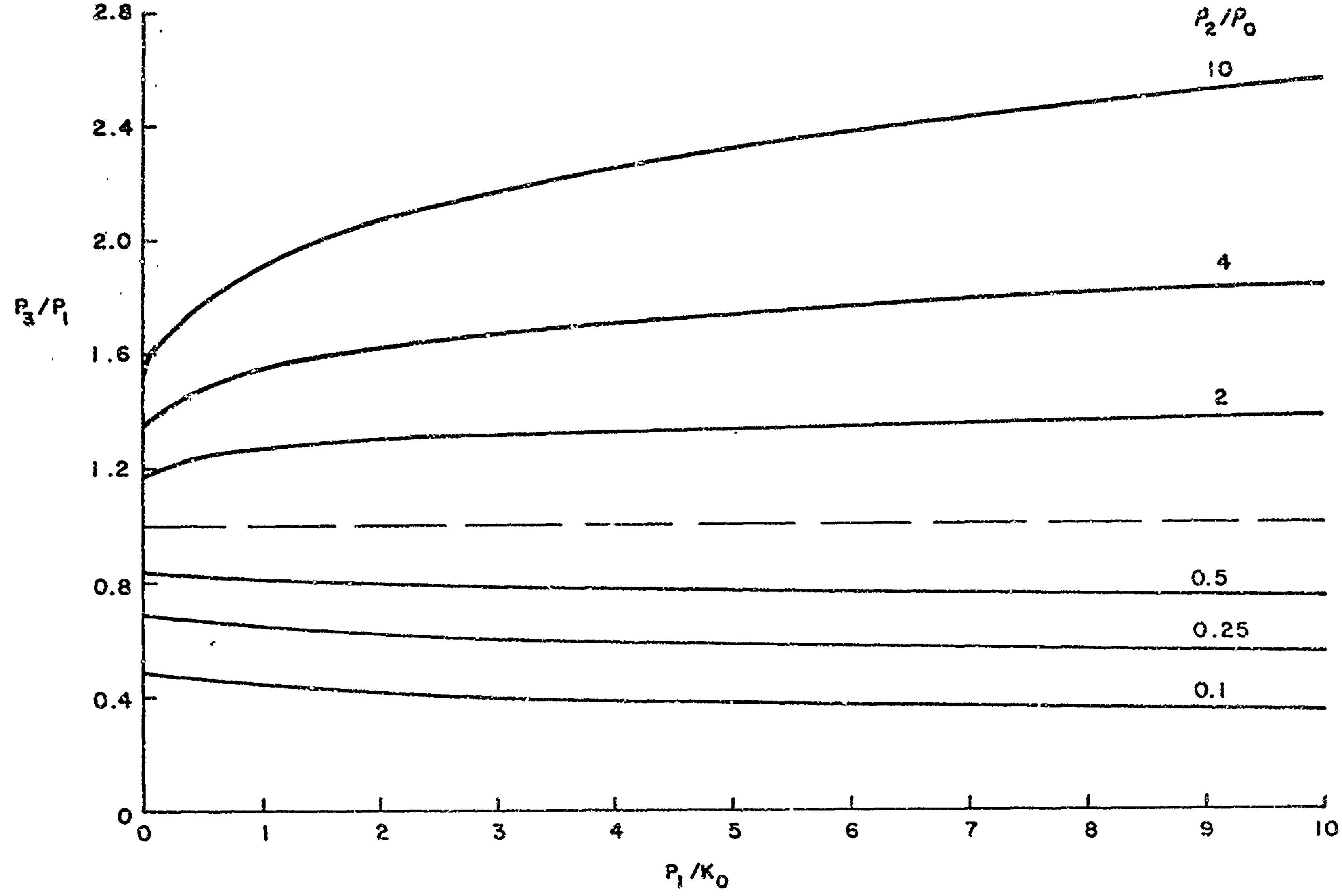

Fig. 9--The ratio of transmitted pressure, p_3, to incident pressure, p_1, in the case where the bulk modulus ratio, K_2/K_0 equals 1.

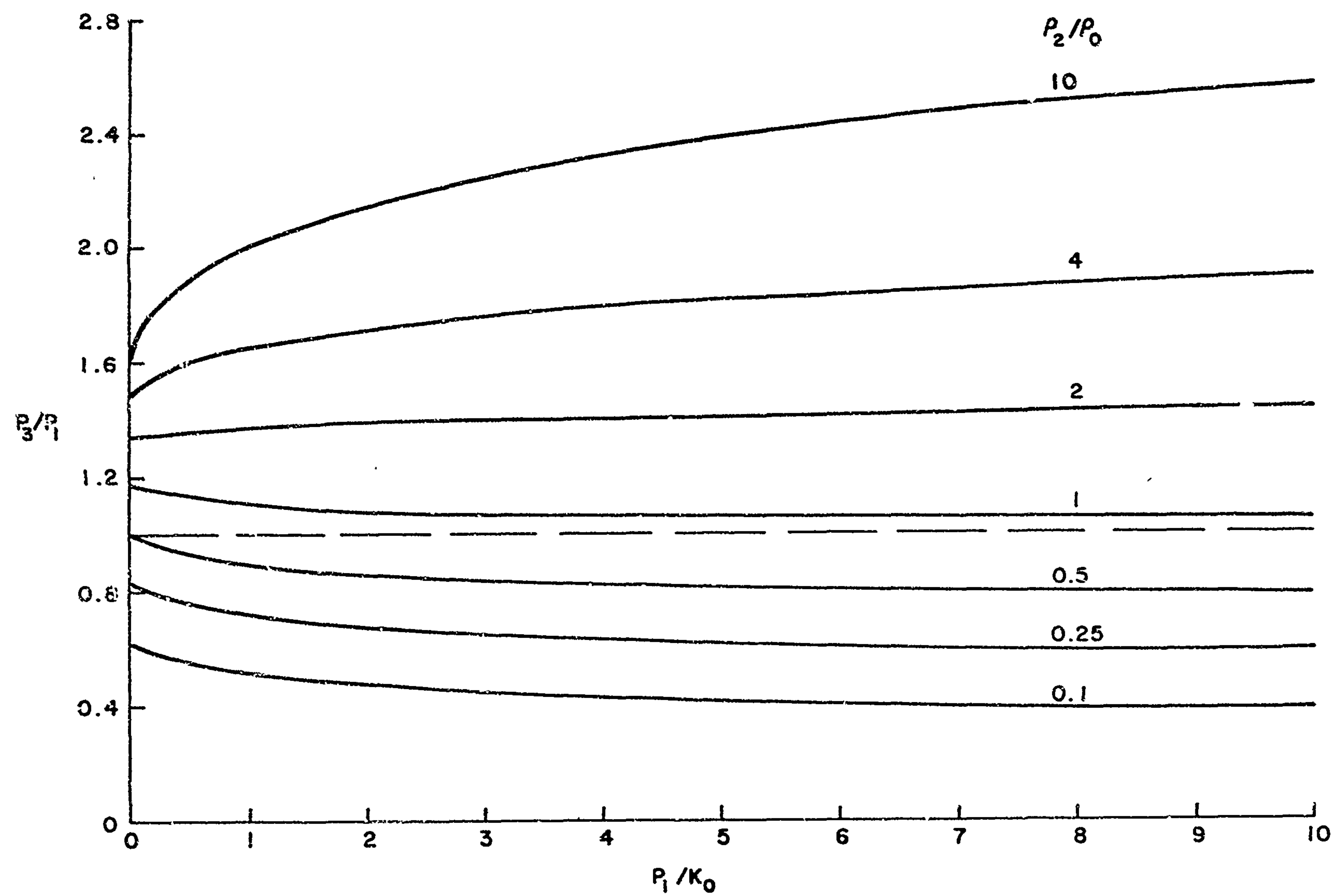

Fig. 10--The ratio of transmitted pressure, p_3, to incident pressure, p_1, in the case where the bulk modulus ratio, K_2/K_0 equals 2.

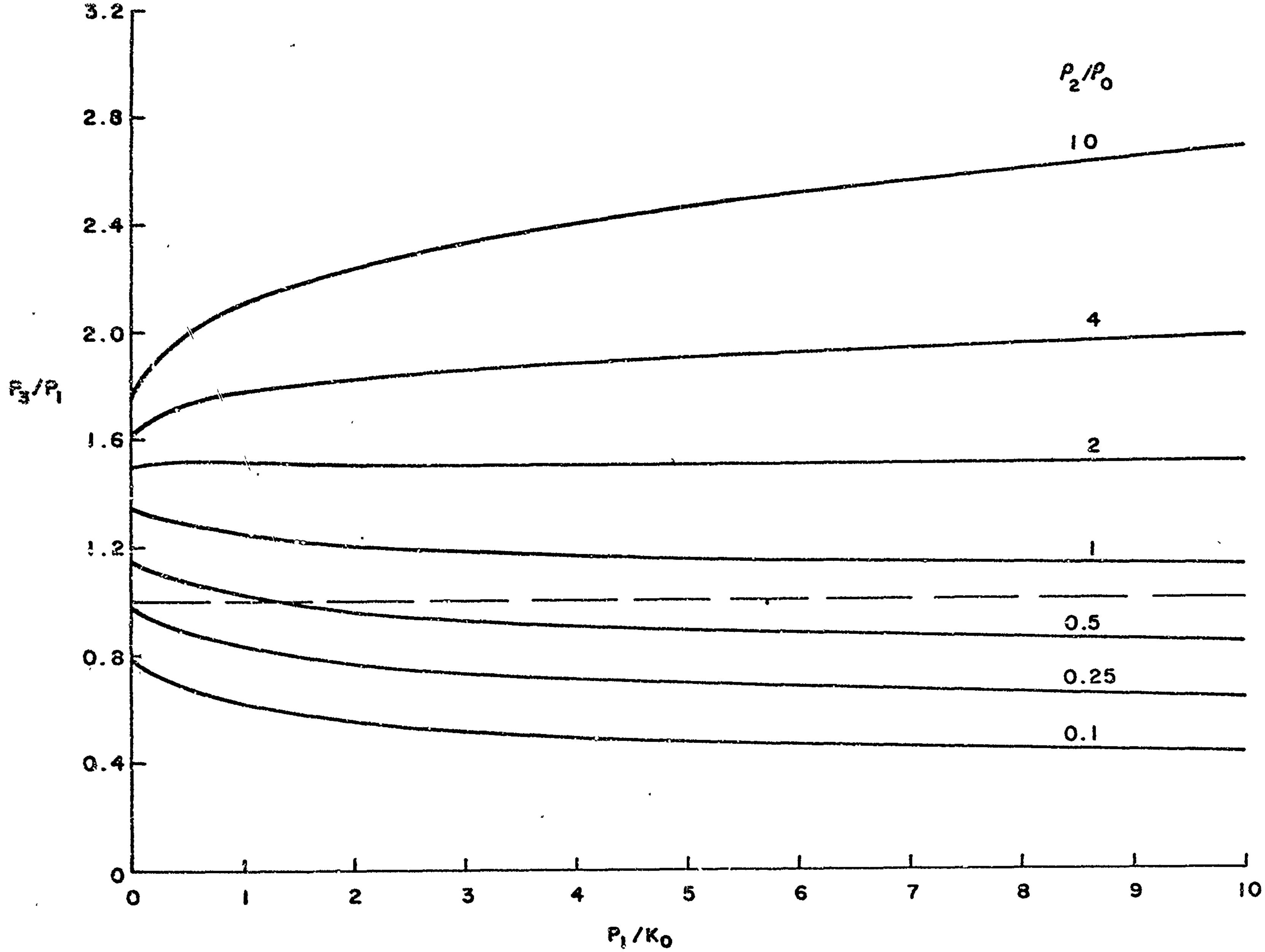

Fig. 11--The ratio of transmitted pressure, p_3, to incident pressure, p_1, in the case where the bulk modulus ratio, K_2/K_0 equals 4.

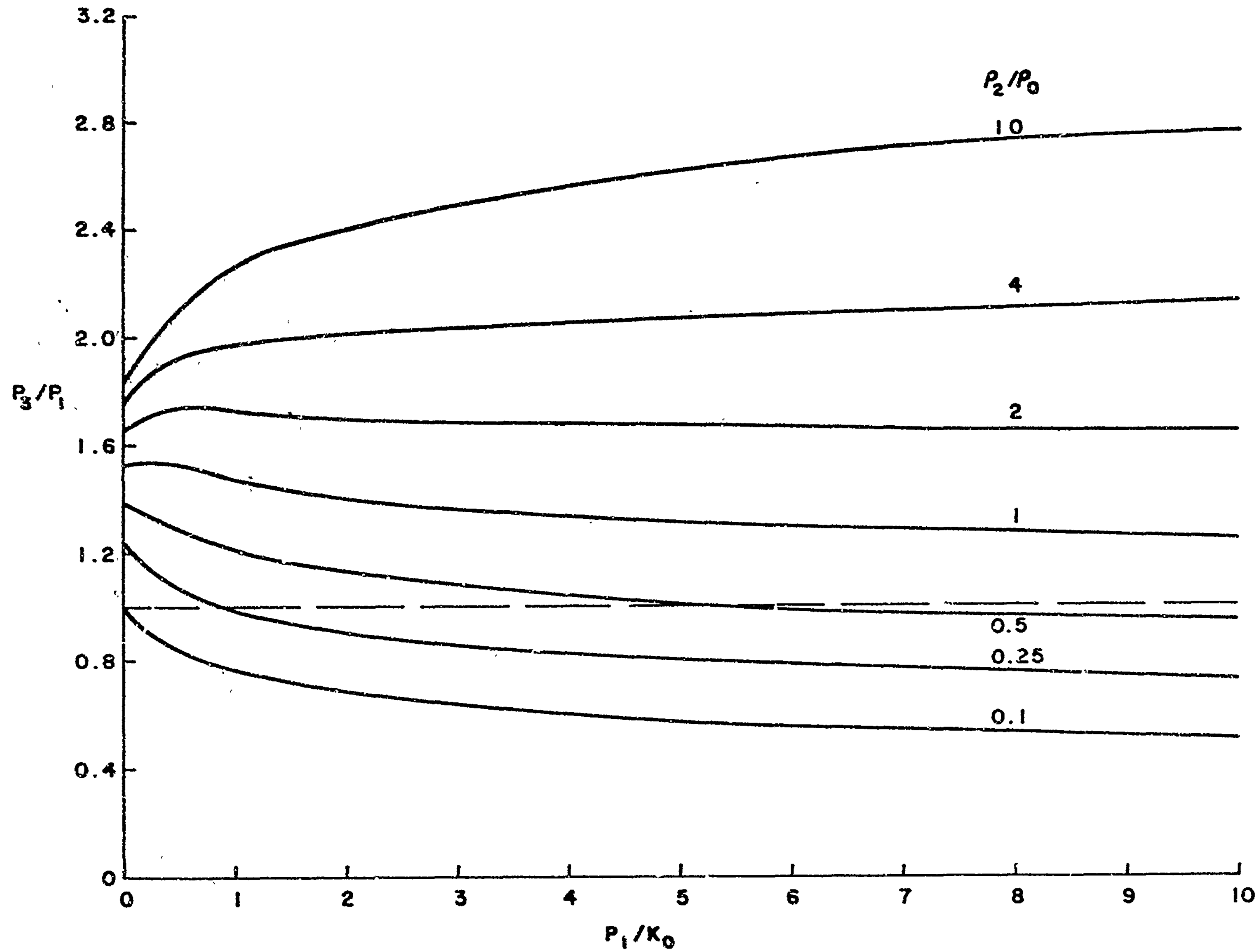

Fig. 12--The ratio of transmitted pressure, p_3, to incident pressure, p_1, in the case where the bulk modulus ratio, K_2/K_0 equals 10.

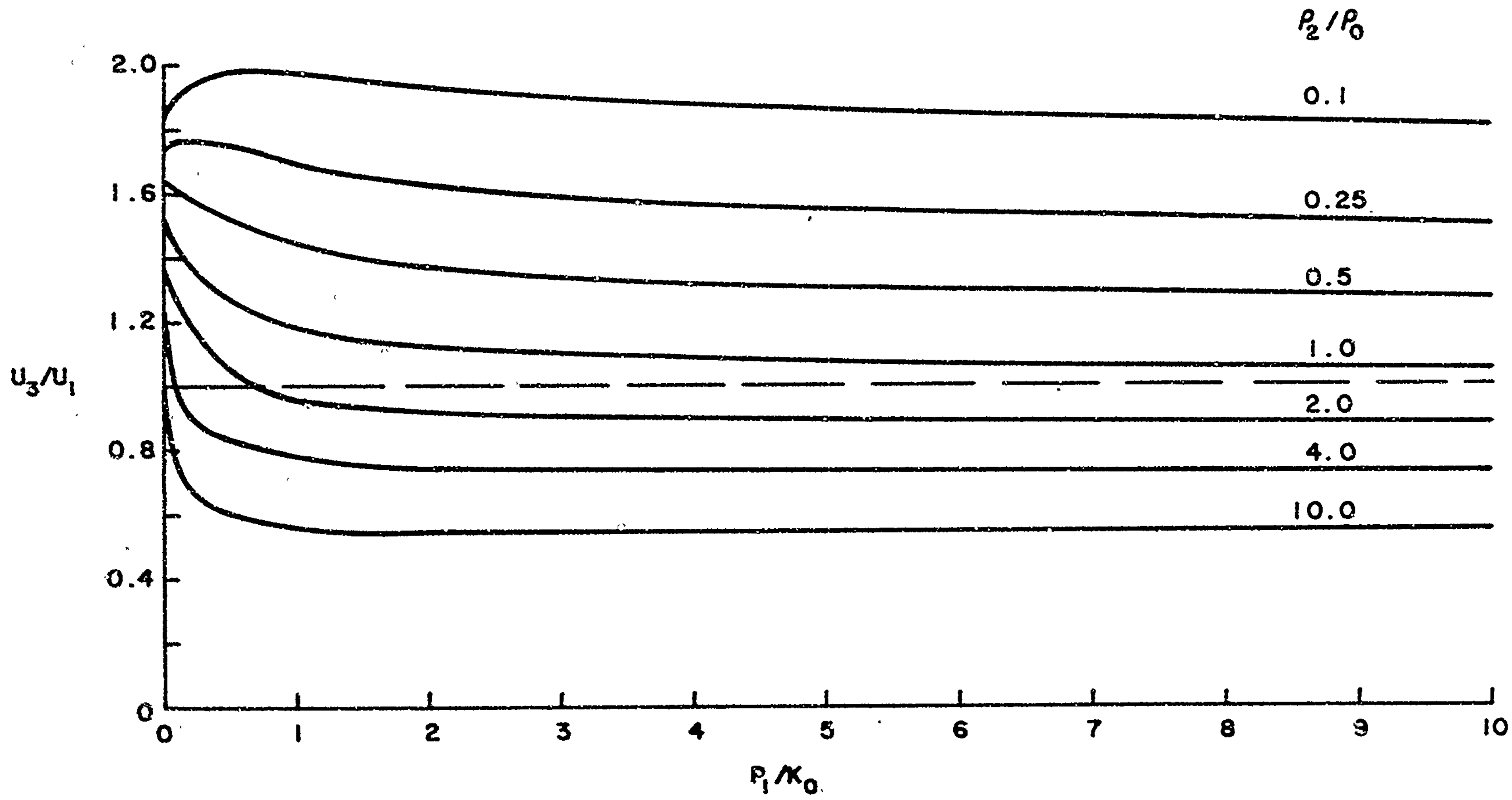

Fig. 13--The ratio of particle velocity in the transmitted wave, u_3, to particle velocity in the incident wave, u_1, in the case where the bulk modulus ratio, K_2/K_0 equals 1/10.

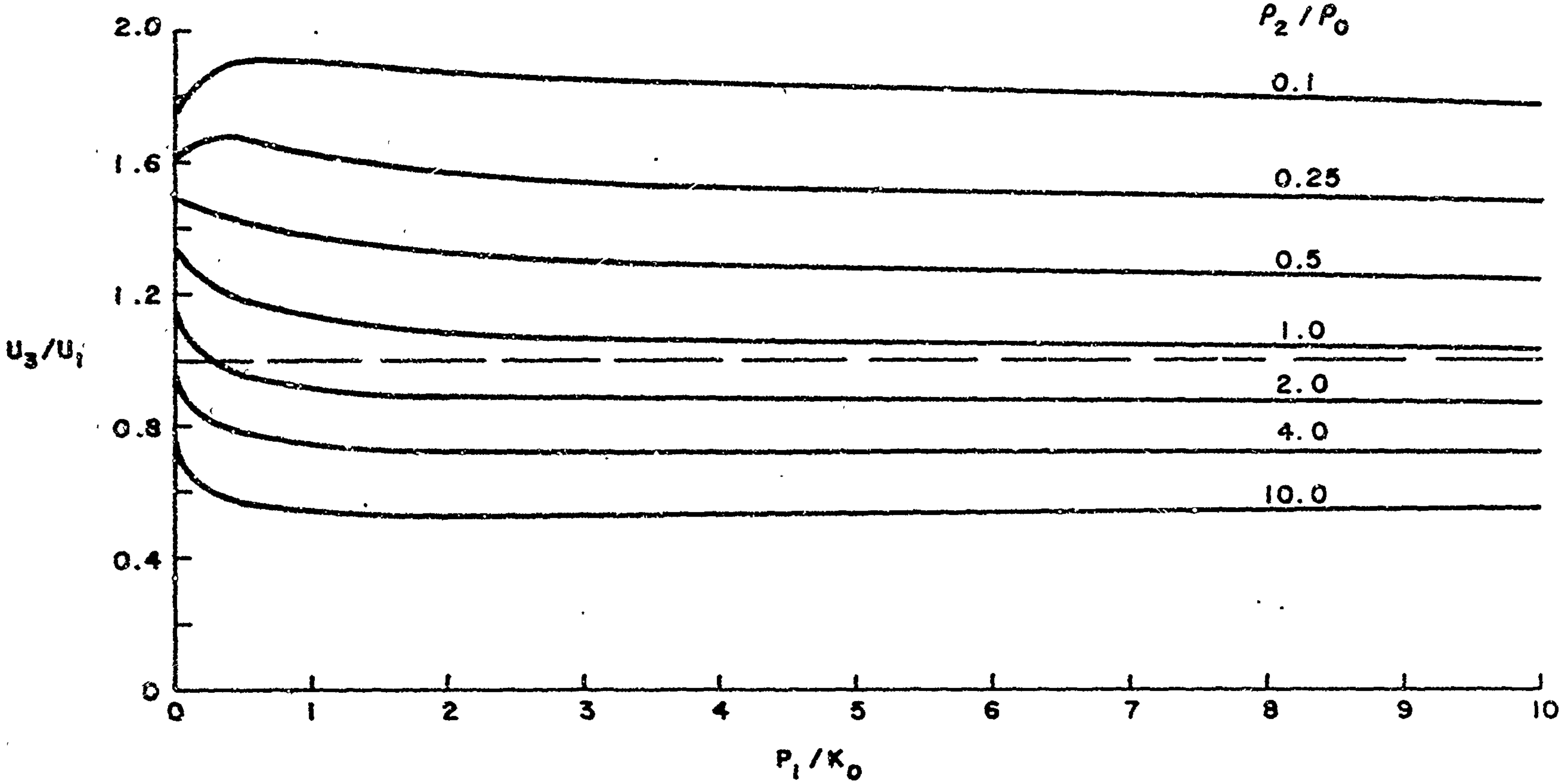

Fig. 14--The ratio of particle velocity in the transmitted wave, u_3, to particle velocity in the incident wave, u_1, in the case where the bulk modulus ratio, K_2/K_0 equals 1/4.

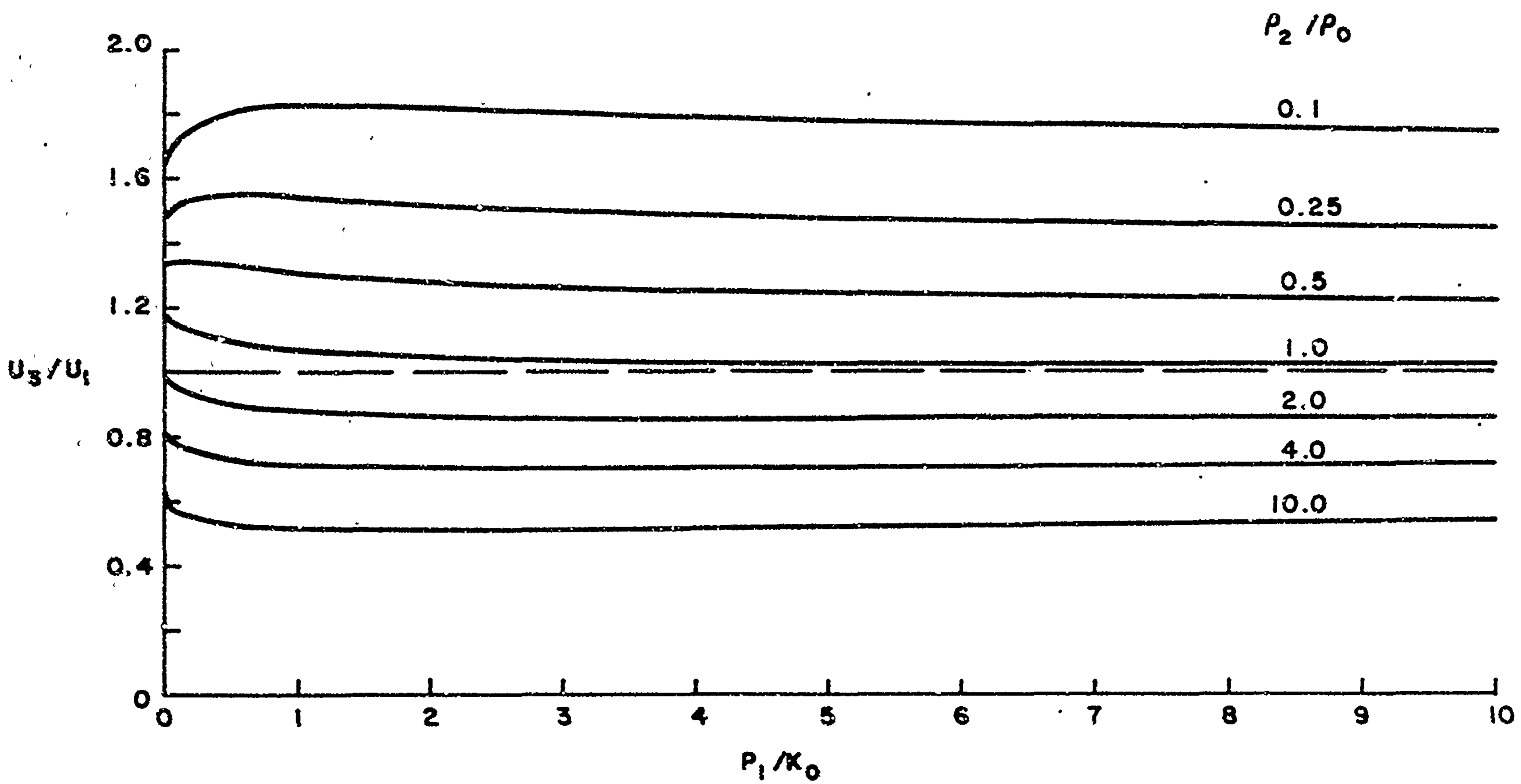

Fig. 15--The ratio of particle velocity in the transmitted wave, u_3, to particle velocity in the incident wave, u_1, in the case where the bulk modulus ratio, K_2/K_0 equals 1/2.

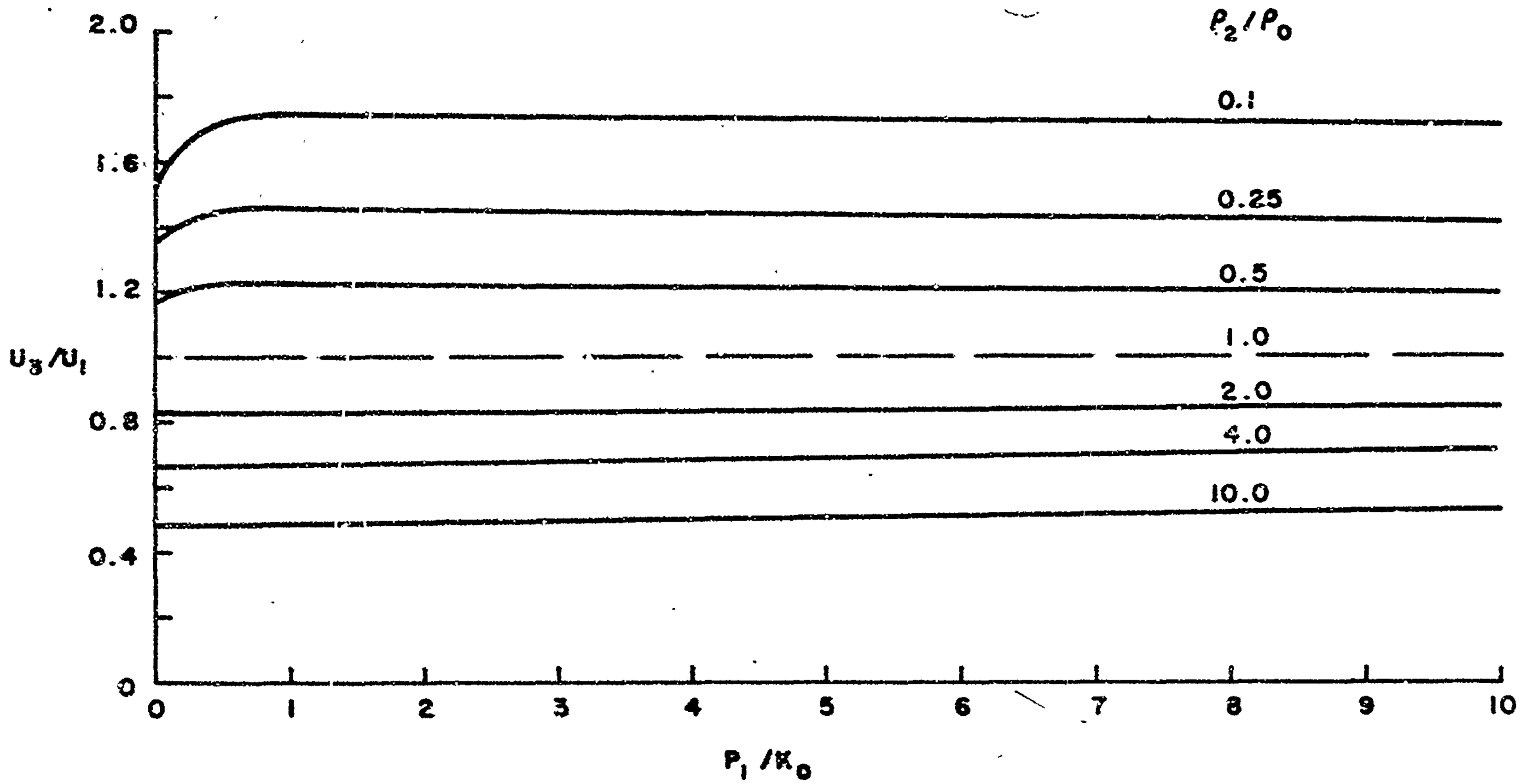

Fig. 16--The ratio of particle velocity in the transmitted wave, u_3, to particle velocity in the incident wave, u_1, in the case where the bulk modulus ratio, K_2/K_0 equals 1.

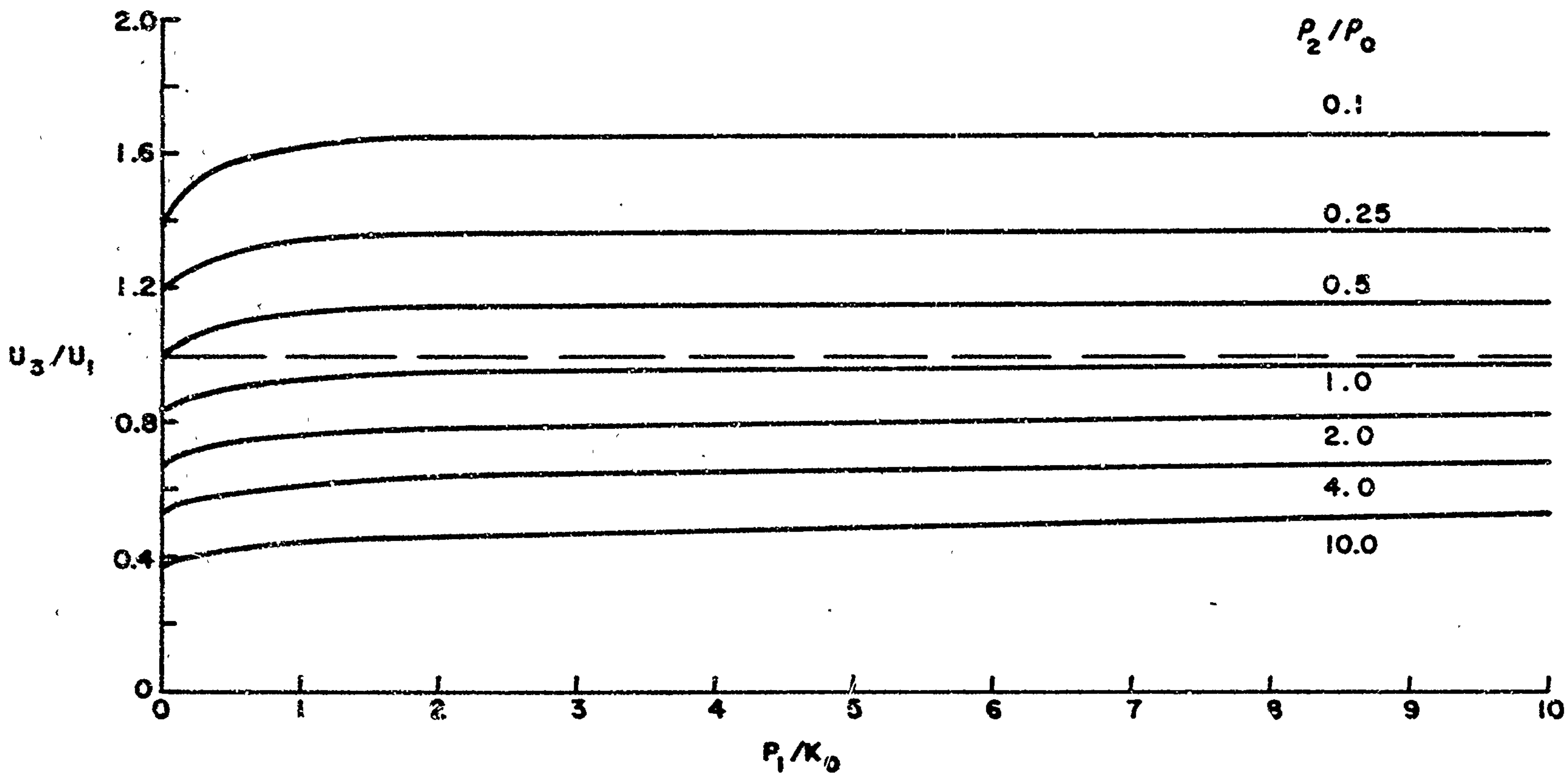

Fig. 17--The ratio of particle velocity in the transmitted wave, u_3, to particle velocity in the incident wave, u_1, in the case where the bulk modulus ratio, K_2/K_0 equals 2.

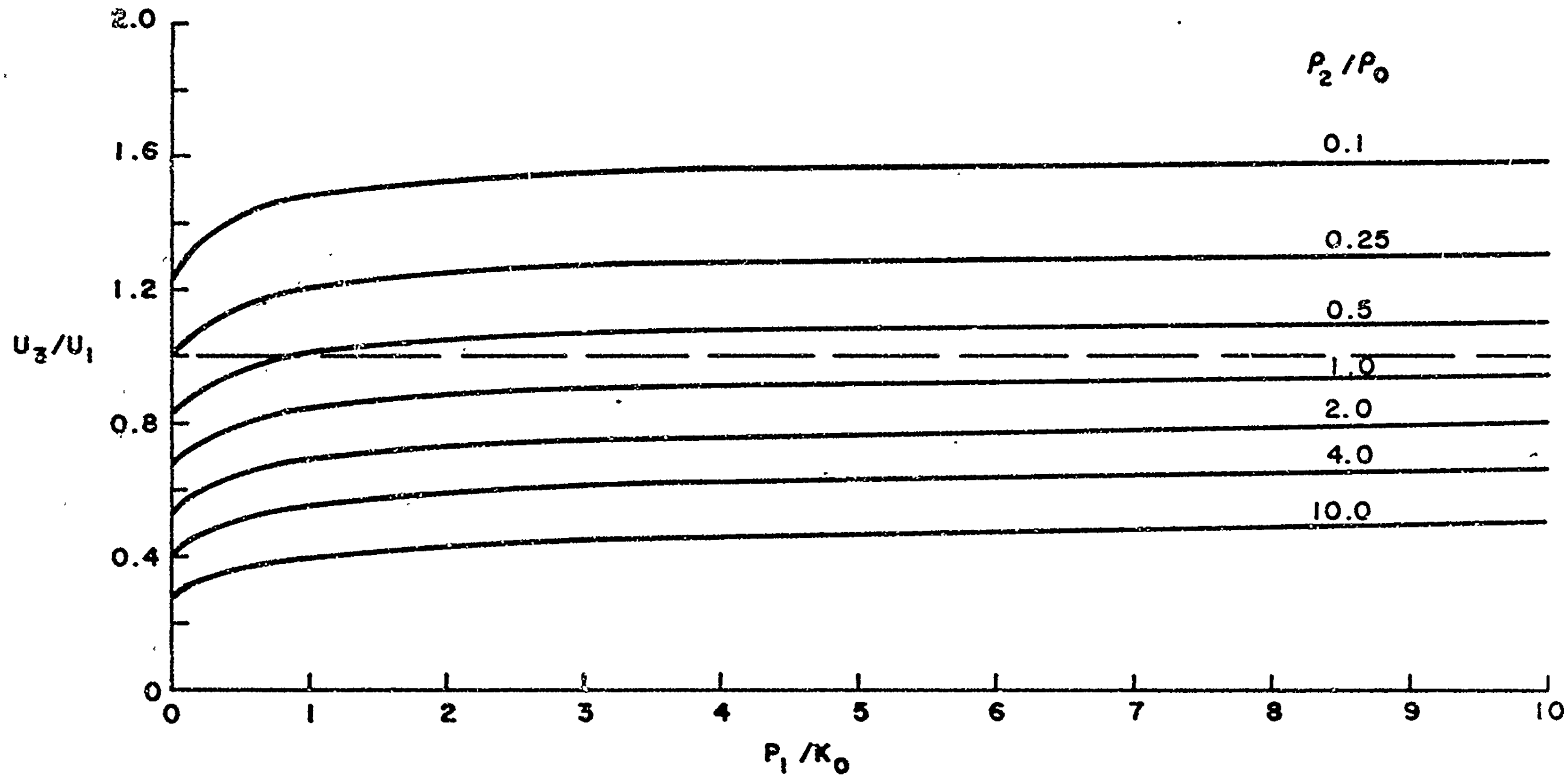

Fig. 18--The ratio of particle velocity in the transmitted wave, u_3, to particle velocity in the incident wave, u_1, in the case where the bulk modulus ratio, K_2/K_0, equals 4.

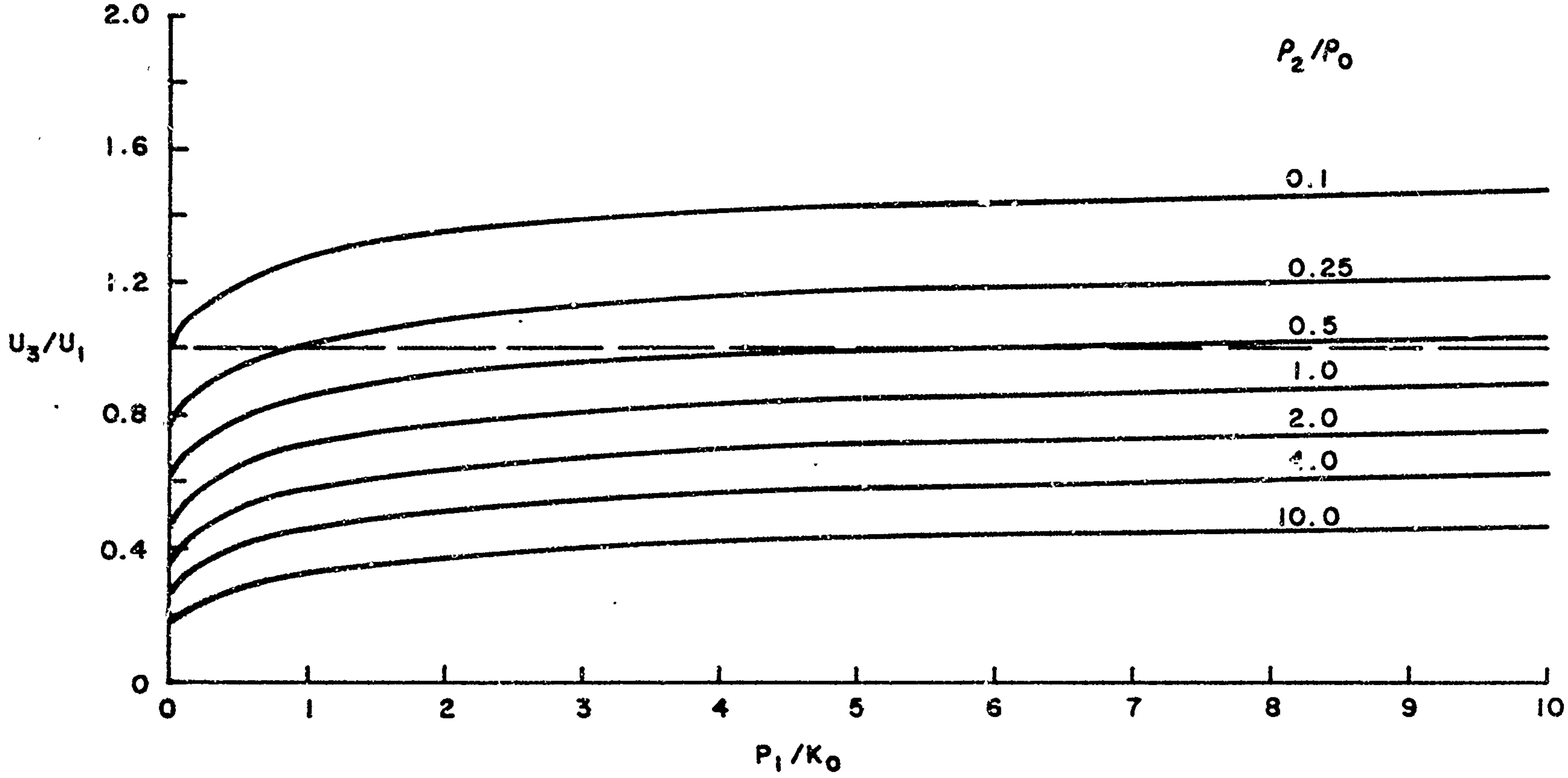

Fig. 19--The ratio of particle velocity in the transmitted wave, u_3, to particle velocity in the incident wave, u_1, in the case where the bulk modulus ratio, K_2/K_0 equals 10.

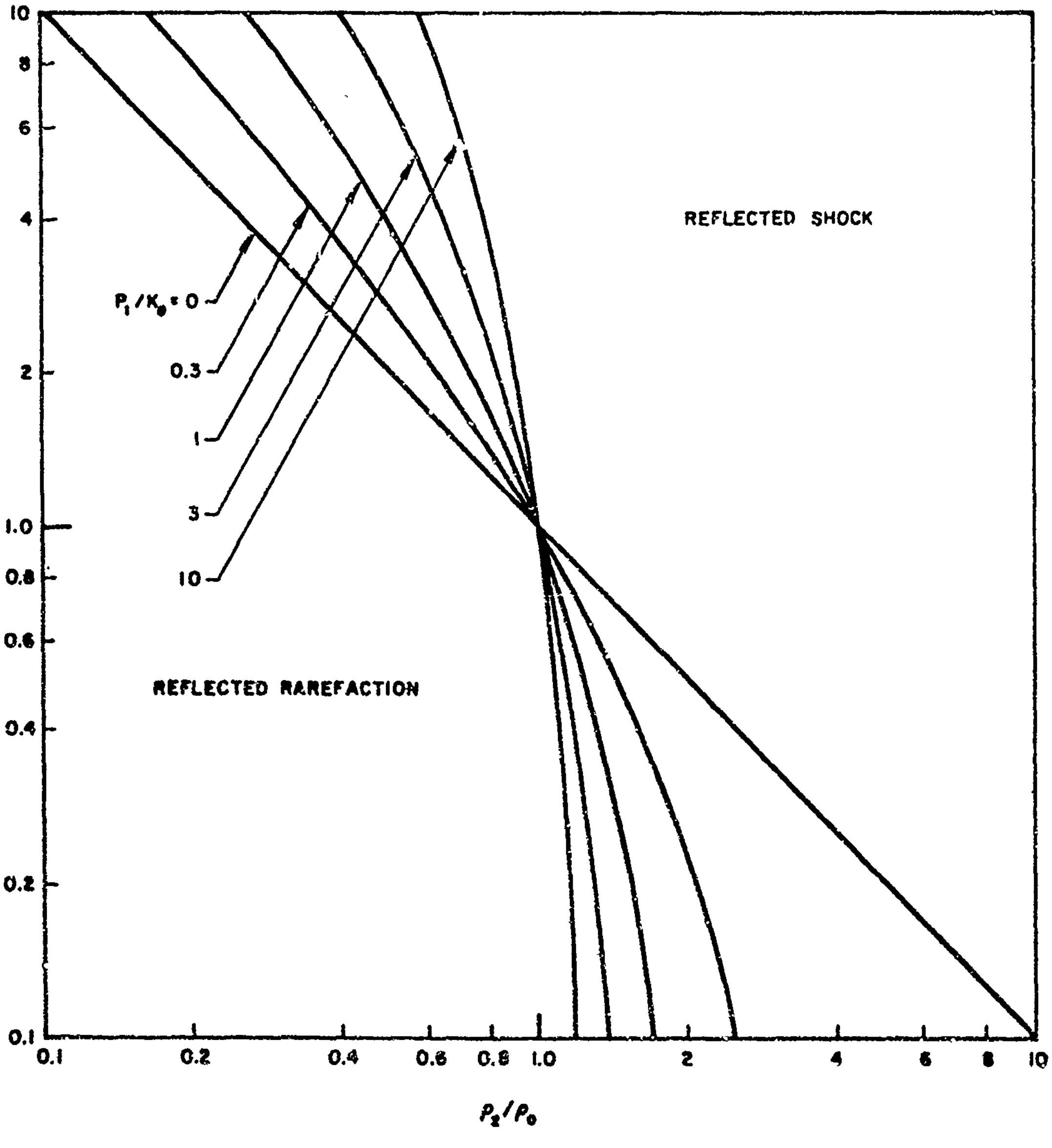

Fig. 20--The boundary between the reflected shock case and the reflected rarefaction case as a function of bulk modulus ratio, K_2/K_0, and density ratio, ρ_2/ρ_0. The boundary depends on shock strength, $\bar{p}_1$, which is expressed in units of the bulk modulus, K_0, in the diagram. If the parameters are such that a point lies on the boundary there is no reflected wave.

REFERENCES

1. Courant, R. and K. O. Friedrichs, Supersonic Flow and Shock Waves, Interscience Publishers, New York, 1948, p. 153.

2. McQueen, R. G. and S. P. Marsh, "Equation of State for 19 Metallic Elements from Shock Wave Measurements to Two Megabars," J. Appl. Physics, July 1960, pp. 1253-1269.

3. Tillotson, J. H., "Metallic Equations of State for Hypervelocity Impact," General Atomic Report GA-3216, July 18, 1962.

4. Cohen, A., Differential Equations, D. C. Heath and Co., 1933, Ch. XIII.